ELSEVIER

J. Non-Newtonian Fluid Mech. 102 (2002) 321–342

Journal of Non-Newtonian Fluid Mechanics

www.elsevier.com/locate/jnnfm

Effect of viscous heating on linear stability of viscoelastic cone-and-plate flow: axisymmetric case

David O. Olagunju [a,*], L. Pamela Cook [a], Gareth H. McKinley [b]

[a] *Department of Mathematical Sciences, University of Delaware, Newark, DE 19716, USA*
[b] *Department of Mechanical Engineering, Massachusetts Institute of Technology, Cambridge, MA 02139, USA*

Abstract

The effect of viscous heating on the linear stability of torsional flow of a viscoelastic fluid is analyzed. We consider an Oldroyd-B fluid subjected to a steady shearing motion in a cone–plate system with small gap. Previous experimental and analytical results show that in the isothermal case the flow is unstable to short wavelength disturbances for values of the Deborah number greater than some critical value. In this paper we show that viscous heating, which is characterized by a radially averaged Nahme number, $\widetilde{Na}$, has a stabilizing effect on both long wave and short wave disturbances. This is in qualitative agreement with experimental results of Rothstein and McKinley [Phys. Fluids 13 (2001) 382].

Keywords: Viscous heating; Linear stability; Viscoelastic cone-and-plate flow

1. Introduction

In this paper the effect of viscous heating on the stability of viscoelastic cone-and-plate flow is investigated. The analysis assumes that the cone angle, α is small as is typical in rheometric devices. In order to make the analysis tractable we also assume that the Nahme–Griffith number Na (which provides a dimensionless measure of the viscous heating relative to conduction) is small. Although this assumption is made for mathematical convenience, the small Nahme number limit has some practical significance as well. For example Turian and Bird [2] showed that the calculated values of the torque on the plate showed appreciable deviation from experimentally measured values if $Na \simeq 0.1$. In some recent experimental work conducted by Rothstein and McKinley [1], the Nahme number spanned the range from 10^{-3} to 1.0. Our analysis shows that viscous heating has a stabilizing effect on the cone-and-plate flow of a viscoelastic fluid governed by the Oldroyd-B constitutive equation. In addition, the nature of the instability is found to be unchanged from the isothermal case. This is the same conclusion arrived at experimentally

* Corresponding author.
E-mail address: olagunju@math.udel.edu (D.O. Olagunju).
Dedicated to Professor Acrivos on the occasion of his retirement from the Levich Institute and the CCNY.

0377-0257/02/$ – see front matter
PII: S0377-0257(01)00185-9

by Rothstein and McKinley [1]. In [3], Becker and McKinley found that although plane Couette flow is always stable, viscous heating tended to destabilize moderate to long wave length disturbances, while short wavelength disturbances tended to be stabilized.

This conclusion is quite different from that obtained in both numerical and experimental investigations of Taylor–Couette flow. In this curvilinear geometry, viscous heating is found to destabilize the flow as a result of a coupling between velocity perturbations and radial temperature gradients arising from viscous dissipation in the base flow [4]. This coupling results in a lower critical Deborah number and also leads to a different mode of instability. In contrast to the time-dependent non-axisymmetric disturbances expected from isothermal analysis, the most unstable perturbations are found to be axisymmetric and steady in time, in better agreement with experimental observations using ideal elastic fluids [5]. Non-linear analysis further shows that the new thermoelastic mode of instability is typically overstable in time, in contrast to the subcritical Hopf bifurcation predicted from isothermal analysis [6]. These findings are robust for a wide range of rheological parameters and constitutive models [7]. However, the existence and parametric location of this new thermoelastic mode is very sensitive to other features such as the symmetry of the base flow. For example, in pressure-driven Taylor–Dean flow of elastic fluids, viscous heating is predicted to monotonically stabilize the isothermal viscoelastic instability and computations suggest that the new disturbance mode is only important at very large values of the Peclet number [8]. The experimental measurements with elastic fluids in torsional flows in [1] also demonstrate a strong monotonic stabilizing effect arising from internal viscous dissipation. As a consequence of the rheometric importance of the cone-and-plate geometry, the effects of viscous heating on both steady [2,9] and oscillatory shear flows [10] of inelastic fluids have been studied analytically in some detail; however, the impact of thermal effects on the purely elastic instabilities that also arise in this torsional flow have not been considered to date. In the present paper we analyze this interaction of fluid viscoelasticity, streamline curvature and viscous dissipation using a non-isothermal formulation of the Oldroyd-B constitutive model.

2. Governing equations

We consider the non-isothermal flow of an incompressible viscoelastic fluid in the gap between a flat plate and an inverted cone with angle α. The fluid is subjected to a shearing motion by rotating the cone at a constant angular speed ω. For small α, the effect of inertia is negligible and the dimensionless equations governing the flow are the continuity equation,

$$\nabla \cdot \boldsymbol{v} = 0, \tag{2.1}$$

and the momentum equation

$$0 = -\nabla p + \nabla \cdot \{(1-\beta)\mathrm{e}^{-\vartheta}\dot{\boldsymbol{\gamma}} + \boldsymbol{\tau}\}, \tag{2.2}$$

where $\dot{\boldsymbol{\gamma}}$ is the rate of strain tensor and $\boldsymbol{\tau}$ is the extra stress arising from the polymer. The retardation parameter β is the ratio of polymer viscosity to the zero-shear rate viscosity at some reference temperature. For non-isothermal flows described by the Oldroyd-B constitutive model, the pseudo time hypothesis [11] can be used to show that the extra stress $\boldsymbol{\tau}$, satisfies the equation

$$\boldsymbol{\tau} + De_0 \frac{\mathrm{e}^{-\vartheta}}{(1+\vartheta/\delta)}\left(\frac{\mathrm{D}\boldsymbol{\tau}}{\mathrm{D}t} - \boldsymbol{L}\cdot\boldsymbol{\tau} - \boldsymbol{\tau}\cdot\boldsymbol{L}^{\mathrm{T}} - \boldsymbol{\tau}\frac{\mathrm{D}}{\mathrm{D}t}\ln\left(1+\frac{\vartheta}{\delta}\right)\right) = \beta\,\mathrm{e}^{-\vartheta}\dot{\boldsymbol{\gamma}}, \tag{2.3}$$

where $\boldsymbol{L}$ is the dimensionless velocity gradient tensor, while the energy equation is

$$Pe\frac{\mathrm{D}\vartheta}{\mathrm{D}t} = \nabla^2\vartheta + Na_0[(1-\beta)\mathrm{e}^{-\vartheta}\dot{\boldsymbol{\gamma}} + \boldsymbol{\tau}] : \nabla\boldsymbol{v}. \tag{2.4}$$

The boundary conditions are no-slip on the solid plates, and constant temperature, $\hat{T} = \hat{T}_\mathrm{p}$ at the flat plate and $\hat{T} = \hat{T}_\mathrm{c}$ at the cone. We use carets to explicitly denote a dimensional quantity. In the following analysis we will ignore the effect of the free surface; for analysis of free surface effects in torsional flow see [12–15]. In the equations above, we have non-dimensionalized length by the plate radius R, velocity by $R\omega$, time by $1/\omega$, pressure and stresses by $\eta_0\omega$, and temperature by a reference temperature $\hat{T}_0$. The quantity η_0 is the zero-shear rate viscosity at the reference temperature $\hat{T}_0$ while the variable ϑ is related to the dimensionless temperature T by

$$\vartheta = \delta(T-1).$$

Here, δ is the dimensionless thermal sensitivity

$$\delta = \frac{\hat{T}_0}{\eta_0}\left|\frac{\partial\eta}{\partial\hat{T}}\right|_{\hat{T}=\hat{T}_0}. \tag{2.5}$$

This thermal sensitivity is typically large for polymeric fluids so that even small variations in T lead to O(1) changes in ϑ. For polyisobutylene-based liquids experiments [16] suggest $\delta_\mathrm{PIB} \simeq 20$ and for polystyrene-based elastic fluids [1], $\delta_\mathrm{PS} \simeq 60$. Due to viscous heating, the viscosities and fluid relaxation time are both strongly temperature dependent. In this paper these have been modeled as in [3] by a Nahme type law. The solvent and polymer viscosities are given, respectively, by

$$\eta_\mathrm{s} = \eta_{\mathrm{s}0}\,\mathrm{e}^{-\vartheta}, \qquad \eta_\mathrm{p} = \eta_{\mathrm{p}0}\,\mathrm{e}^{-\vartheta},$$

and the relaxation time by

$$\lambda = \lambda_0\frac{\mathrm{e}^{-\vartheta}}{(1+\vartheta/\delta)},$$

where $\eta_{\mathrm{s}0}$, $\eta_{\mathrm{p}0}$ and λ_0 are, respectively, the solvent viscosity, polymer viscosity and relaxation time at the reference temperature $\hat{T}_0$.

The parameters in Eqs. (2.1)–(2.4) are the retardation parameter $\beta = \eta_{\mathrm{p}0}/\eta_0$, the Nahme number $Na_0 = \eta_0\delta R^2\omega^2/(\hat{k}\hat{T}_0)$, and the Deborah number $De_0 = \lambda_0\omega$, at the reference temperature, and the Peclet number $Pe = c_\mathrm{p}\rho R^2\omega/\hat{k}$. Here $\hat{k}$ is the thermal conductivity of the fluid and $\eta_0 = \eta_{\mathrm{s}0} + \eta_{\mathrm{p}0}$. Another parameter of interest that is sometimes used in the analysis of non-isothermal flows is the Brinkman number Br, which is related to the Nahme number by $Br = Na/\delta$. In later sections we introduce another parameter $\mathcal{P}$ which is the ratio of the Peclet number to the Deborah number.

A principal reason why the cone–plate system is a popular rheometric design is the fact that for α small, the shear rate $\tau_{\phi\theta}$ is approximately constant. If $Na \neq 0$, the shear rate is no longer homogeneous. However, if the Nahme number is small the deviation from homogeneity is also small and O(Na). Since we are principally interested in rheometric flows, and also to simplify the analysis, we will assume that Na is small. Some of the experiments of Rothstein and McKinley [1] were conducted at very low temperatures and spanned Nahme numbers from 10^{-3} to 1.0, so this restriction is a reasonable one. For these elastic fluids the parameter $\mathcal{P}$ is also small (typically of the order O(10^{-1})), therefore we will assume that $\mathcal{P}$ is negligible in most of our numerical computations.

3. Base flow

We use a spherical coordinate system (r, ϕ, θ) and for convenience we scale ϕ as follows:

$$\phi = \tfrac{1}{2}\pi - \alpha\psi,$$

so that $\psi = 0$ at the plate and $\psi = 1$ on the surface of the cone. We assume that the cone angle α is small enough that terms of order $O(\alpha^2)$ can be neglected. Nominally, the thermal boundary conditions at the upper cone and lower plate are held at a fixed temperature, say ϑ_w. However in most rheometric devices only the stationary (lower) fixture is actually thermostated (using for example a Peltier element). The freely-rotating upper fixture is assumed to be close to constant temperature due to the large thermal mass and high thermal conductivity of the constituent material. Al-Mubaiyedh et al. [6,7] show that even small changes in the thermal boundary condition ($\pm 1\,^\circ$C) can have large changes in the stability characteristics of non-isothermal viscoelastic Taylor–Couette flow. To investigate the sensitivity of viscoelastic torsional flow to non-homogeneous thermal boundary conditions, we consider boundary conditions of the form $\vartheta = \vartheta_w$ at the plate, and $\vartheta = \vartheta_w + r^2\, Na_0\, e^{-\vartheta_w}\mu$ at the cone. Note that ϑ_w is not necessarily the same as the reference condition $\vartheta = 0$. Also, note that these conditions correspond not to an externally imposed temperature difference $\Delta\hat{T}$ but rather an induced temperature difference arising from viscous heating in the torsional base flow. The magnitude of μ in reality would be determined from modeling of the heat transfer from the fluid to the cone and the resulting conduction and convection through the rotating fixture. Although we present results for positive and negative values of μ, in practice we would only expect $\mu > 0$.

As in [2,3], for $\mu = 0$ a steady torsional solution is given by

$$\upsilon_r = \upsilon_\phi = 0, \qquad \upsilon_\theta = \frac{r}{2}\left(1 + \frac{[\tanh c(2\psi - 1)]}{\tanh c}\right), \tag{3.1}$$

$$\tau_{rr} = \tau_{r\phi} = \tau_{\phi\phi} = 0, \tag{3.2}$$

$$\tau_{r\theta} = \beta\, e^{-\vartheta}\left(\frac{\partial \upsilon_\theta}{\partial_r} - \frac{\upsilon_\theta}{r}\right), \tag{3.3}$$

$$\tau_{\theta\phi} = -\frac{\beta}{\alpha}\, e^{-\vartheta}\left(\frac{1}{r}\frac{\partial \upsilon_\theta}{\partial \psi}\right), \tag{3.4}$$

$$\tau_{\theta\theta} = \frac{2\beta De_0}{\alpha^2}\frac{e^{-2\vartheta}}{(1 + \vartheta/\delta)}\left(\frac{1}{r}\frac{\partial \upsilon_\theta}{\partial \psi}\right)^2, \tag{3.5}$$

and

$$\vartheta = \vartheta_w + \ln\left(\frac{\operatorname{sech}^2[c(2\psi - 1)]}{\operatorname{sech}^2 c}\right), \tag{3.6}$$

where

$$c = \sinh^{-1}\left(r\sqrt{\frac{Na}{8}}\right).$$

Here, the rescaled Nahme number at the wall temp ϑ_w is defined by

$$Na = e^{-\vartheta_w} Na_0,$$

and $\vartheta_w = \delta(T_w - 1)$. The solution given by Eqs. (3.1)–(3.6), must satisfy the remaining momentum equations which are

$$\frac{\partial p}{\partial r} = \frac{\tau_{\theta\theta}}{r}, \qquad \frac{\partial p}{\partial \psi} = \alpha \tan(\alpha\psi)\tau_{\theta\theta}. \tag{3.7}$$

If $De = 0$ so that $\tau_{\theta\theta} = 0$, Eq. (3.7) is compatible and the solution reduces to those obtained by Turian and Bird [2]. For $De \neq 0$, Eq. (3.7) is not compatible in general. In order for these two equations to be compatible however, the Nahme number must be small. Specifically, it is necessary that terms of O(Na^2), and O(Br) be negligible.

Neglecting terms of order O(α^2; Na^2; αNa) and O(Br), the solution for $\mu \neq 0$ obtained by a regular expansion is given by,

$$\upsilon_\theta = r\psi\left[1 + \tfrac{1}{12} r^2 Na\, \psi(1-\psi)(2\psi - 1 - 6\mu)\right], \tag{3.8}$$

$$p = \frac{-2\beta\, e^{-\vartheta_w} De}{\alpha^2}\left(\ln r - \frac{1+6\mu}{12} r^2 Na\right), \tag{3.9}$$

$$\tau_{r\theta} = \tfrac{1}{6} r^2 \beta\, e^{-\vartheta_w} Na\, \psi(1-\psi)(2\psi - 1 - 6\mu), \tag{3.10}$$

$$\tau_{\phi\theta} = e^{-\vartheta_w} \frac{\beta}{\alpha}\left(1 - \frac{1+6\mu}{12} r^2 Na\right), \tag{3.11}$$

$$\tau_{\theta\theta} = \frac{2e^{-\vartheta_w}\beta\, De}{\alpha^2}\left(1 - \frac{1+6\mu}{6} r^2 Na\right), \tag{3.12}$$

and

$$\vartheta = \vartheta_w + \tfrac{1}{2} r^2 Na\, \psi(1 - \psi + 2\mu). \tag{3.13}$$

The scaled perturbations to the base velocity and temperature fields due to viscous heating are shown in Fig. 1. Specifically, we have plotted w and χ defined by $w = Na^{-1}\langle \upsilon_\phi - r\psi \rangle$ and $\chi = Na^{-1}\langle \vartheta - \vartheta_w \rangle$ where $\langle\cdot\rangle$ denotes a radially averaged quantity. Viscous heating in the base shear flow leads to a spatially varying tangential velocity with a cubic correction of O(Na) as in plane Couette flow [2,3]. The temperature perturbation consists of a quadratic variation across the gap due to viscous heating in the fluid superposed with a linear variation of magnitude μ arising from the possible non-homogeneity in the thermal boundary conditions. The temperature dependent Deborah number at the wall reference temperature is given by

$$De = e^{-\vartheta_w} \frac{De_0}{(1 + \vartheta_w/\delta)}. \tag{3.14}$$

It can be seen from Fig. 1(b) that for $\mu < 0$ the average temperature across the gap will be significantly lower than ϑ_w and thus the Deborah number will be higher than this value. The converse is true for $\mu > 0$. These changes in the effective measure of elasticity in the fluid affect the stability boundaries as we show below.

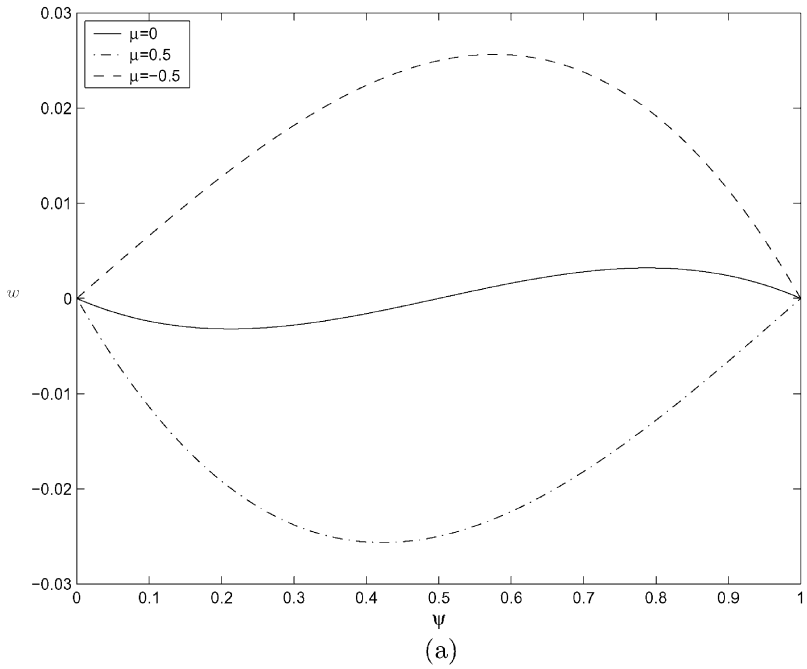

Fig. 1. Deviation of base velocity (a) and temperature profiles (b) from their isothermal values for selected values of μ.

Setting $De = 0$ and $\beta = 0$ in Eqs. (3.8)–(3.13), we obtain to order O(Na) the perturbation result of Turian and Bird [2]. They showed that the calculated values of the torque on the plate showed appreciable deviation from experimentally measured values even at $Na \simeq 0.1$. This is further justification for taking $Na \ll 1$. Similar perturbation solutions were obtained by Turian [9] for non-Newtonian fluids governed by the power law and the Ellis constitutive equation.

4. Linear stability

We now proceed to study the linear stability of the base flow given by Eqs. (3.8)–(3.13). Denote by $\boldsymbol{q}$, the vector of unknowns

$$\boldsymbol{q} = [\upsilon_r, \upsilon_\phi, \upsilon_\theta, p, \tau_{rr}, \tau_{r\phi}, \tau_{r\theta}, \tau_{\phi\phi}, \tau_{\phi\theta}, \tau_{\theta\theta}, \vartheta],$$

and by $\bar{\boldsymbol{q}}$, the base flow obtained in the previous section. Let

$$\boldsymbol{q} = \bar{\boldsymbol{q}} + \boldsymbol{q}',$$

where $\boldsymbol{q}'$ is a small perturbation. We then linearize about the base flow and obtain equations for the perturbations. A solution of the linearized equations is sought in the form

$$\boldsymbol{q}' = \exp(\sigma t)[\upsilon_r', \upsilon_\phi', \upsilon_\theta', \ldots, \vartheta'],$$

where $\upsilon_r', \upsilon_\phi', \ldots, \vartheta'$ are functions of r and ψ. The resulting equations can be solved for the stresses. Substituting these in the continuity and momentum equations, and eliminating the pressure, we are left with four equations for the velocity disturbances, $\upsilon_r', \upsilon_\phi', \upsilon_\theta'$, and the temperature perturbation ϑ'. These equations depend on the local value of the Nahme number $r^2\,Na$ at a radial location r and hence are not separable. However, if Na is small, then the variation in the local Nahme number will also be small. Therefore, in order to facilitate the analysis, we will replace the local Nahme number with its average value $\widetilde{Na} = \int_0^1 r^3\,Na\,\mathrm{d}r / \int_0^1 r\,\mathrm{d}r$, then the coefficients are independent of r.

We then seek solutions in the form

$$\begin{pmatrix} \upsilon_r' \\ \upsilon_\phi' \\ \upsilon_\theta' \\ \vartheta' \end{pmatrix} = r^{\mathrm{i}k} \begin{pmatrix} rQ_0' \\ rQ_1' \\ r\,De\,Q_2' \\ De\,Q_3' \end{pmatrix},$$

where we have denoted perturbed quantities with a tilde and $Q_j' = Q_j'(\psi)$ for $j = 0 - 3$. The equation of continuity to leading order in α is given by

$$\alpha(3 + \mathrm{i}k)\,Q_0' - \frac{\partial Q_1'}{\partial \psi} = 0. \tag{4.1}$$

For $\alpha \ll 1$, we see from Eq. (4.1) that the two limits of interest are $k = \mathrm{O}(1)$, and $k = \mathrm{O}(\alpha^{-1})$. For the case $k = \mathrm{O}(1)$, we scale $Q_1' = \alpha Q_1$, and for the short wavelength case we scale the wave number $k = \kappa/\alpha$ where $\kappa = \mathrm{O}(1)$. Solving Eq. (4.1) for Q_0' and substituting in the remaining three equations

and dropping all the primes, we obtain to leading order in α the following coupled system of equations for Q_1, Q_2, and Q_3.

$$A_4\frac{\partial^4 Q_1}{\partial\psi^4}+A_3\frac{\partial^3 Q_1}{\partial\psi^3}+A_2\frac{\partial^2 Q_1}{\partial\psi^2}+A_1\frac{\partial Q_1}{\partial\psi}+A_0Q_1+B_2\frac{\partial^2 Q_2}{\partial\psi^2}+B_1\frac{\partial Q_2}{\partial\psi}+B_0Q_2 + C_1\frac{\partial Q_3}{\partial\psi}+C_0Q_3=0, \tag{4.2}$$

$$D_2\frac{\partial^2 Q_2}{\partial\psi^2}+D_1\frac{\partial Q_2}{\partial\psi}+D_0Q_2+E_2\frac{\partial^2 Q_1}{\partial\psi^2}+E_1\frac{\partial Q_1}{\partial\psi}+E_0Q_1+F_1\frac{\partial Q_3}{\partial\psi}+F_0Q_3=0, \tag{4.3}$$

and

$$H_2\frac{\partial^2 Q_3}{\partial\psi^2}+H_0Q_3+G_1\frac{\partial Q_1}{\partial\psi}+G_0Q_1+K_1\frac{\partial Q_2}{\partial\psi}=0. \tag{4.4}$$

The boundary conditions are

$$\frac{\mathrm{d}Q_1}{\mathrm{d}\psi}=Q_1=0, \quad \text{for } \psi=0,1, \tag{4.5}$$

$$Q_2=Q_3=0, \quad \text{for } \psi=0,1. \tag{4.6}$$

The coefficients in the above equations are given in Appendix A. In addition to the parameters β, De, and $\widetilde{Na}$, the equations also depend on the new parameter $\mathcal{P}$ defined as

$$\mathcal{P}=\frac{\rho c_\mathrm{p}(\hat{r}\alpha)^2}{\hat{k}\lambda_0}=\frac{t_\mathrm{thermal}}{t_\mathrm{polymer}},$$

a ratio of the thermal diffusion time scale to the polymeric time scale. This parameter is purely a function of material and geometric quantities and can also be written as $\mathcal{P}=Pr/E$ where Pr is the Prandtl number and E is the elasticity number. $\mathcal{P}$ can also be expressed as the $\mathcal{P}=Pe/De$ where Pe is the Peclet number and De is the Deborah number. For the elastic fluids studied by Rothstein and McKinley [1], $\mathcal{P}\sim \mathrm{O}(10^{-1})$. Note that $\mathcal{P}$ scales quadratically with the geometric size; for large geometries or moderately elastic fluids $\mathcal{P}\geq 1$ as in the experiments of White and Muller [5]. This ratio is important in transient problems and governs which thermophysical property approaches steady state most rapidly. The temperature field evolves on the time scale t_thermal and the viscoelastic stresses on the time scale t_polymer. Exploratory stability calculations for $0<\mathcal{P}<100$ show that the value of P does not qualitatively affect the stability characteristics of the steady non-isothermal viscoelastic torsional flow; therefore in the subsequent analysis we will typically set $\mathcal{P}=0$ when computing numerical results.

4.1. Moderate wave numbers, $k=O(1)$

As mentioned above, for this case $Q_1'=\mathrm{O}(\alpha)$. Thus, we introduce the scaling $Q_1'=\alpha Q_1$ in the momentum equations to obtain Eqs. (4.2)–(4.4) above. For the isothermal case, $Na=0$, Eq. (4.4) reduces to

$$\frac{\partial^2 Q_3}{\partial\psi^2}-\mathcal{P}\Omega Q_3=0, \tag{4.7}$$

together with the boundary conditions $Q_3(0) = Q_3(1) = 0$ where Ω is related to the dimensionless growth rate σ by $\Omega = De\,\sigma$. If $\mathcal{P} \neq 0$, this problem has non-trivial solutions if and only if $\Omega = -(n\pi)^2\mathcal{P}$ where n is an integer. Since $\Omega < 0$, these solutions are always stable. This is to be expected since Q_3 represents perturbations to the temperature field. With no viscous heating the heat equation is unconditionally stable. On the other hand if $\mathcal{P}\Omega = 0$, then we have that $Q_3 \equiv 0$ and the energy equation decouples from the momentum and constitutive equations. Solving Eq. (4.3) for Q_2 and substituting in Eq. (4.2) we obtain for the tangential velocity perturbation Q_1 the following eigenvalue problem:

$$\frac{\partial^4 Q_1}{\partial \psi^4} = \Lambda \frac{\partial^2 Q_1}{\partial \psi^2}, \tag{4.8}$$

where the eigenvalue Λ depends on Ω and the parameters De, β and k. It can be shown that the smallest eigenvalue of the problem is given by $\Lambda = 4\pi^2$ [17]. For $k = 0$ the neutral stability curve corresponds to $\Omega = 0$ and is given by

$$De_c = \pi \sqrt{\frac{2}{\beta(3+2\beta)}}. \tag{4.9}$$

This is the critical Deborah number obtained for the class of von Karman similarity solutions by Olagunju and Cook [17]. The linear stability of similarity solutions of isothermal, viscoelastic cone-and-plate flow was first studied by Phan-Thien [18] who showed that for a given value of the parameter β the flow became unstable as the Deborah number increases beyond some critical value. The value of the critical Deborah that he found was later corrected by Olagunju and Cook [17].

To obtain the neutral curve for $k \neq 0$, and for the non-isothermal case we use a Chebychev collocation method as developed by Zebib [19,20] to solve Eqs. (4.2)–(4.4). First, we introduce a new variable $z = 2\psi - 1$ so that the domain is transformed to the interval $-1 \leq z \leq 1$. We then expand the highest derivative for each variable in terms of Chebychev polynomials

$$\frac{\partial^4 Q_1}{\partial z^4} = \sum_{n=0}^{N-1} a_n T_n(z), \tag{4.10}$$

$$\frac{\partial^2 Q_2}{\partial z^2} = \sum_{n=0}^{N-1} b_n T_n(z), \tag{4.11}$$

$$\frac{\partial^2 Q_3}{\partial z^2} = \sum_{n=0}^{N-1} c_n T_n(z). \tag{4.12}$$

Here $T_n(z)$ is the Chebychev polynomial of order n. The expansions for Q_1, Q_2, and Q_3 are obtained by integrating the derivatives given above the required number of times and choosing the constants of integration so that boundary conditions (4.5) and (4.6) are satisfied. The requirement that the problems (4.1)–(4.6) should have non-trivial solutions leads to a generalized eigenvalue problem for the eigenvalue Ω.

$$\mathcal{A}C = \Omega \mathcal{B}C, \tag{4.13}$$

where C is a $3N$ vector of the unknown coefficients a_n, b_n and c_n. The matrices $\mathcal{A}$ and $\mathcal{B}$ are complex and depend on the parameters De, β, $\widetilde{Na}$, $\mathcal{P}$ and the wave number k. The eigenvalue problem is solved using

the IMSL package DGVCCG. The base torsional flow is stable if $\Re(\Omega) < 0$, unstable if $\Re(\Omega) > 0$, and neutrally stable if $\Re(\Omega) = 0$. We fix the parameters β, $\widetilde{Na}$ and $\mathcal{P}$ and obtain for each wave number k, the eigenvalue of Eq. (4.13) with the largest real part as a function of the Deborah number. The critical value of the Deborah number is that at which the real part of the most unstable eigenvalue crosses the imaginary axis into the right half of the complex plane. This gives the neutral stability curve in the *De–k* plane.

4.2. Short wave length limit $k = O(\alpha^{-1})$

In [21], it was shown that for short wavelength perturbations the critical Deborah number scales like $\sqrt{\alpha}$. Therefore, we scale the wave number as $k = \kappa/\alpha$ and the Deborah number as

$$De = \mathcal{D}\sqrt{\alpha}.$$

In addition, we scale the radial and meridional components of velocity as $\tilde{Q}_0 = \alpha Q_0$, and $\tilde{Q}_1 = \alpha Q_1$. Neutral stability curves were obtained as explained above. In the isothermal limit, we recover the results of Olagunju [21].

5. Discussion

Stability results for the moderate wavelength calculations are shown in Fig. 2 for selected values of β and $\widetilde{Na}$. These graphs show that the least unstable perturbations are given by the wave number $k = 0$. As the wave number increases, the critical Deborah number decreases monotonically. In Fig. 3, we plot $\Im(\Omega_c)$, the imaginary part of the scaled growth rate Ω at criticality, as a function of wave number k. For $k = 0$, $\Im(\Omega_c) = 0$ but as k increases, $\Im(\Omega_c)$ also increases monotonically from zero. In addition, for the values of $\widetilde{Na}$ considered, we see that for any given wave number, the critical Deborah number increases with $\widetilde{Na}$, thus showing that moderate to long wave length perturbations are stabilized by viscous heating.

Corresponding results for short wavelength disturbances are depicted in Fig. 4 for selected values of the averaged Nahme number $\widetilde{Na}$, and the retardation parameter β. From these graphs, we see that for each value of the wave number κ there is a value of $\mathcal{D}$ below which the flow is stable and above which it is unstable. The most unstable perturbation corresponds to the minimum point on the neutral stability curve which we will denote $(\kappa_c, \mathcal{D}_c)$. The critical Deborah number is then given by $De_c = D_c\sqrt{\alpha}$. For both the isothermal and non-isothermal cases considered the critical wave number is approximately $(\alpha k)_c \simeq 3.1$. The isothermal result is in agreement with both experimental and analytical results in [21–23]. As in the moderate wave number case, the critical Deborah number increases with $\widetilde{Na}$, indicating that viscous heating also tends to stabilize short wavelength disturbances in good agreement with experiments [1]. For both the upper convected Maxwell and the Oldroyd-B model with $\beta = 0.5$, we find $\mathcal{D}_c = 4.602$ for the isothermal case. This agrees with the result in [21] in which the critical elasticity number was given as $E_c \equiv De_c^2/\alpha = 21.179$. Computed values of $\mathcal{D}_c$ for $\beta = 1.0$ and $\beta = 0.5$ for selected values of $\widetilde{Na}$ are shown in Table 1. While viscous heating tends to stabilize the flow for both values of β considered, the degree of stabilization is greater for $\beta = 1$ than for $\beta = 0.5$. In all cases $\Im(\Omega_c) \neq 0$, but changes very little as a function of the wave number and is an increasing function of $\widetilde{Na}$. For these calculations, terms of order α and δ^{-1} have been neglected.

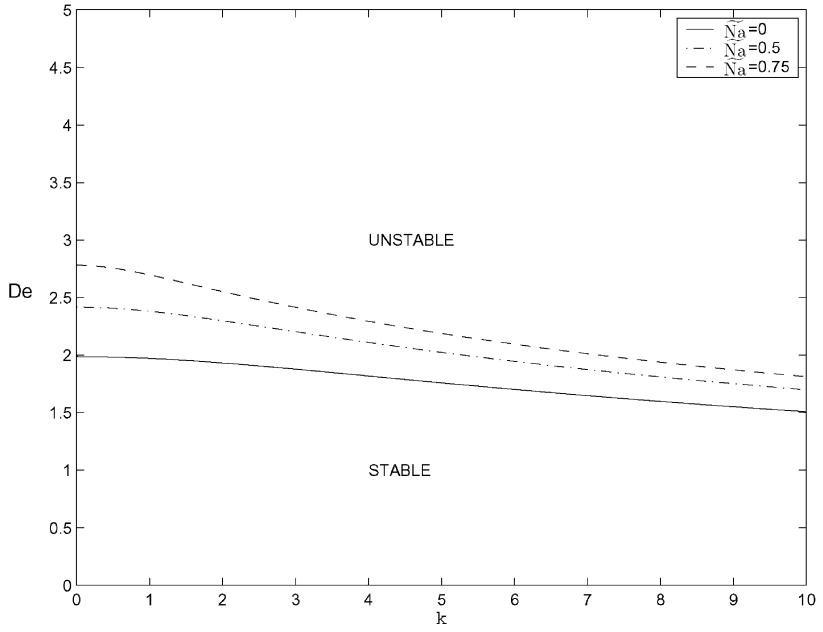

Fig. 2. Neutral stability curve for $\mathcal{P} = 0$ and selected values of $\widetilde{Na}$. (a) $\beta = 1.0$ and (b) $\beta = 0.5$.

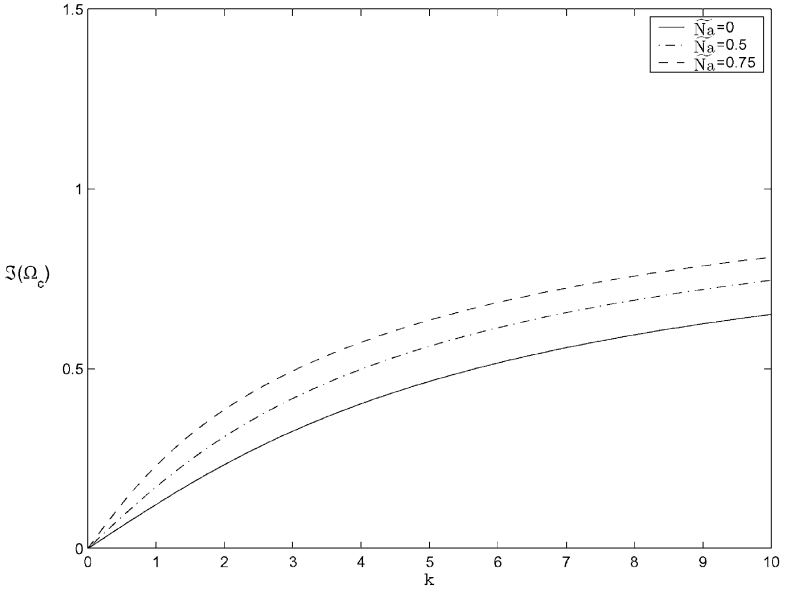

(a)

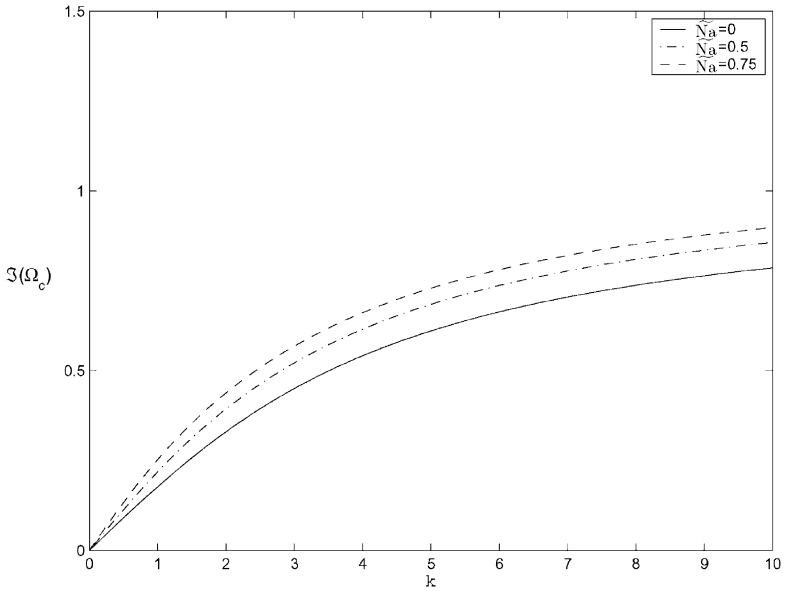

(b)

Fig. 3. $\Im(\Omega_c)$ vs. wave number k for $\mathcal{P} = 0$, and selected values of $\widetilde{Na}$. (a) $\beta = 1.0$ and (b) $\beta = 0.5$.

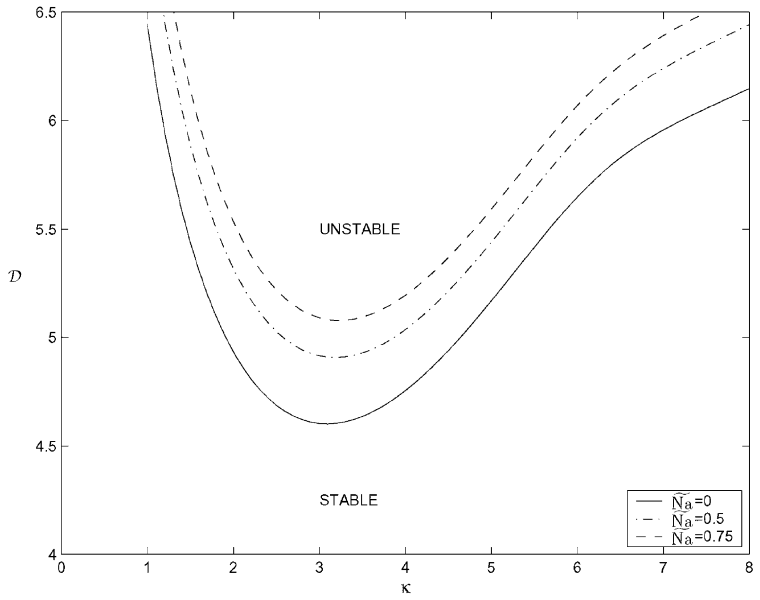

(a)

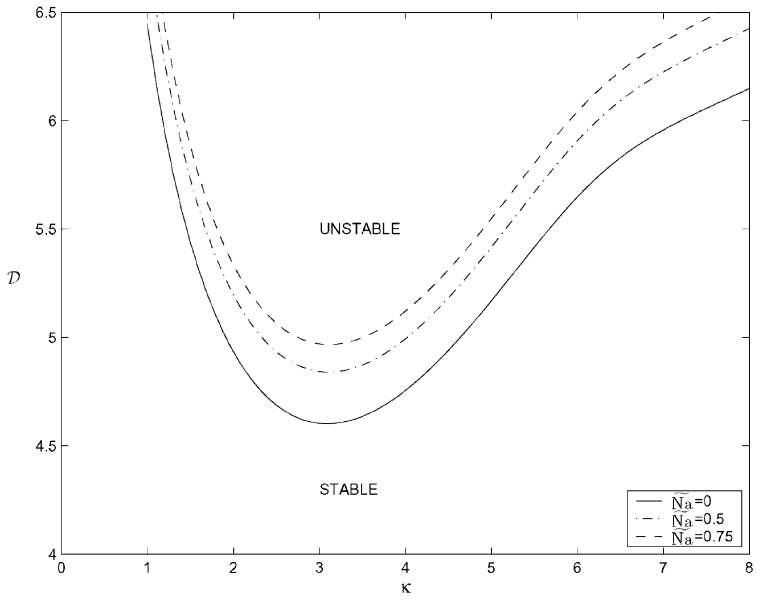

(b)

Fig. 4. Neutral stability curve for $\mathcal{P} = 0$, and selected values of $\widetilde{Na}$. (a) $\beta = 1.0$ and (b) $\beta = 0.5$.

Table 1
Computed values of $\mathcal{D}_c$ for selected values of $\widetilde{Na}$ and β

$\widetilde{Na}$	$\mathcal{D}_c$	
	$\beta = 0.5$	$\beta = 1.0$
0	4.602	4.602
0.5	4.840	4.901
0.75	4.967	5.082

In Fig. 5 we show the variation in the stability boundary for cases in which viscous heating leads to differences in the temperature of the two walls. For $\mu > 0$ the curve is shifted upwards corresponding to a further stabilization in the flow with respect to purely elastic instability. For $\mu < 0$, however, the effects of a linear spatial gradient in the temperature (superimposed on the quadratic variation across the gap due to local viscous dissipation) leads to a destabilization in the flow. A simple interpretation of this phenomenon is to recognize that although the effects of variations in wall temperature on the

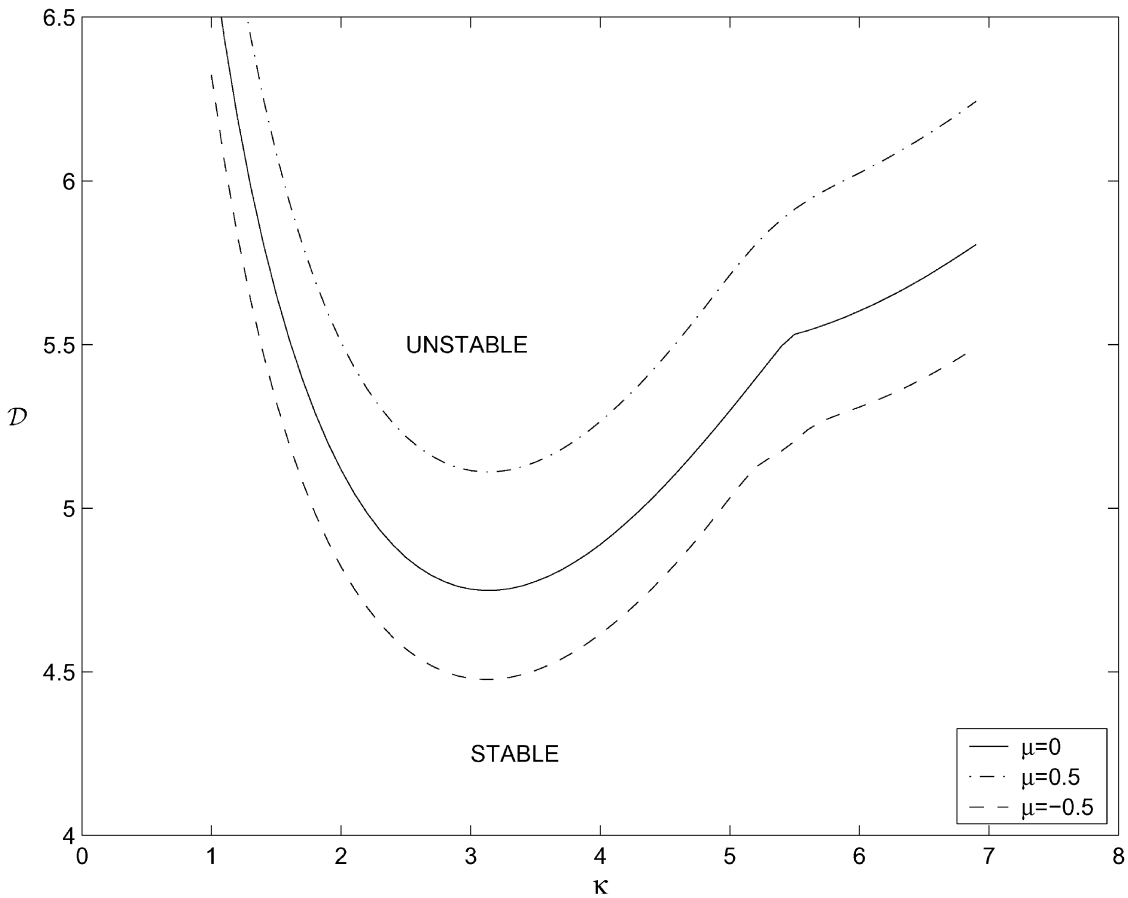

Fig. 5. Neutral stability curve for $\beta = 0.5$, $\mathcal{P} = 0$, $\widetilde{Na} = 0.25$, and selected values of μ.

Deborah number are incorporated (through Eq. (3.14)), the effective or gap-averaged Deborah number will be higher or lower depending on the direction of the temperature variation between the walls. This will lead to an $O(\mu)$ correction, which can be seen in Fig. 5. Very recently, Al-Mubaiyedh et al. [6] have found that small ($\pm 1\,^{\circ}C$) temperature changes in the wall boundary conditions can dramatically change the bifurcation structure (from transcritical to sub- or supercritical Hopf); however we do not see such dramatic changes here. This is because there does not appear to be a new thermoelastic mode for the torsional flow geometry studied here. Viscous heating serves simply to stabilize the isothermal elastic modes that lead to the purely elastic spiral disturbances observed experimentally.

In experimental observations of non-isothermal elastic instabilities, changes in the rotation rate of the fixtures lead to changes in both the Deborah number and the Nahme number. However, the ratio $\sqrt{\widetilde{Na}}/De$ is independent of ω and is only a function of the thermophysical properties of the fluid and the flow geometry. Rothstein and McKinley [1] defined this dimensionless ratio as a thermoelastic number Θ and varied it by performing measurements at different imposed temperatures ϑ_w for a fixed cone angle $\alpha = 2^{\circ}(= \pi/90\,\text{rad})$. In Fig. 6, we plot $\sqrt{\widetilde{Na}}$ versus $\mathcal{D}_c$ for selected values of β. Trajectories for different

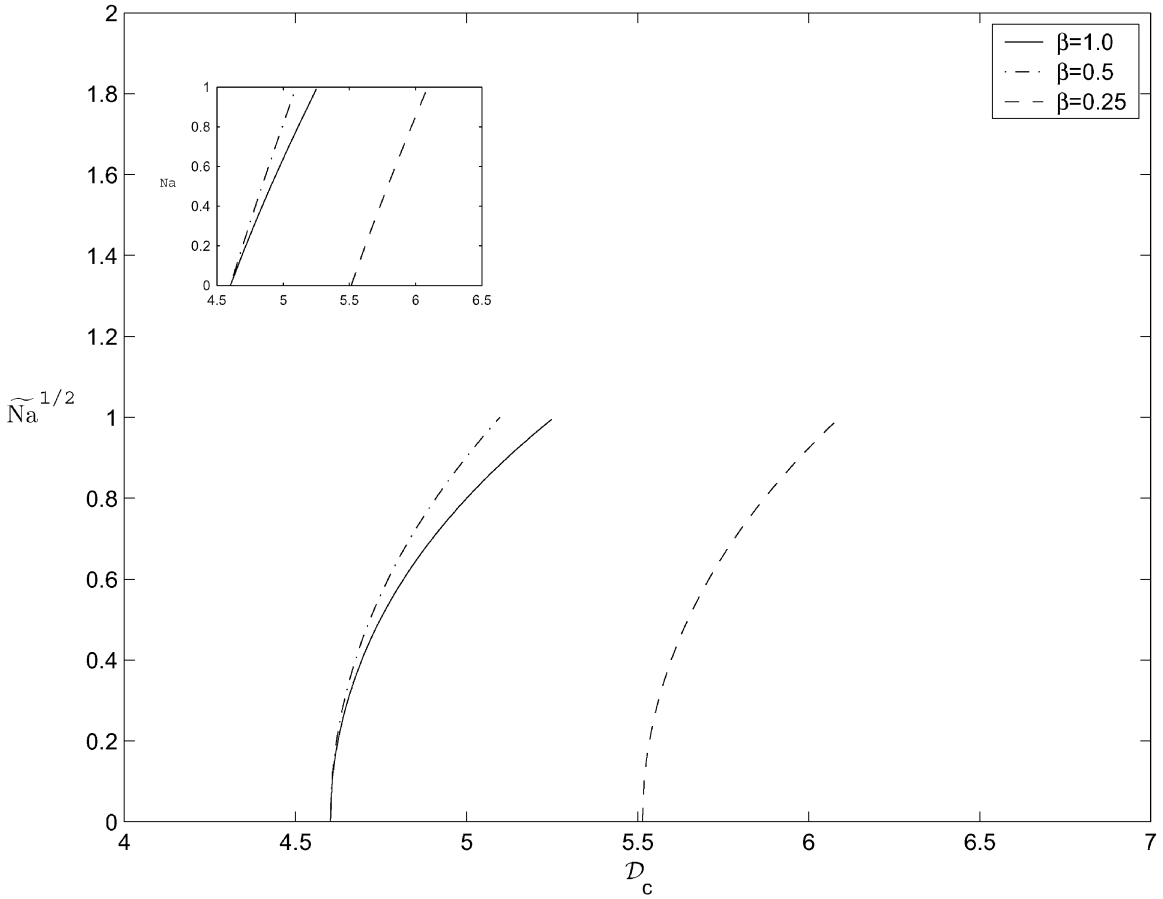

Fig. 6. Plot of $\mathcal{D}_c$ vs. $\widetilde{Na}^{1/2}$ for $\mathcal{P} = 0$, and selected values of β. Insert gives $\mathcal{D}_c$ vs. $\widetilde{Na}$.

values of the thermoelastic parameter correspond, in this space, to lines of slope $\sqrt{\alpha\Theta}$ passing through the origin. Qualitatively, this plot shows very good agreement with that in Rothstein and McKinley [1] with a progressive stabilization as the effects of viscous heating become increasingly important. Although the results reported here are for $\mathcal{P} = 0$, our calculations show that increasing the value up to $\mathcal{P} = 100$ did not change the stability results. Calculations with other values of the retardation parameter β, give similar results as those reported here. In terms of the conditions at the reference temperature, the critical Deborah number is given by

$$\mathcal{D}_c \equiv \frac{\lambda(\hat{T}_w)\omega_c}{\sqrt{\alpha}} = \frac{(\lambda_0 \, e^{-\vartheta_w})\omega_c}{(1 + \vartheta_w/\delta)\sqrt{\alpha}}, \tag{5.1}$$

where the numerical value of $\mathcal{D}_c$ depends on both β and Θ and can be obtained from Fig. 6. For a given value of $\mathcal{D}_c$, the critical rotation rate for the onset of instability depends on the wall temperature T_w.

The results in Fig. 6 show that viscous heating monotonically stabilizes the torsional flow of elastic liquids in cone-and-plate rheometers. Careful examination of the coefficients in Appendix A and the shape of the computed profiles suggest that the critical Deborah number in fact varies with the parameters plotted on the axes in Fig. 6 as $\sqrt{\widetilde{Na}} = K\sqrt{\mathcal{D}_c - \mathcal{D}_{c0}}$. This can be expressed more simply as $\widetilde{Na} = K^2(\mathcal{D}_c - \mathcal{D}_{c0})$ where the constant K is, in fact, also a weak function of the retardation parameter β. The inset to Fig. 6 shows that this linear relationship between $\widetilde{Na}$ and $\mathcal{D}_c$ holds true for all values of β considered. Re-examination of the data in [1] shows that experimental stability measurements in ideal elastic fluids also follow a linear relationship between Na and De_c. In terms of the original dimensional variables, the critical rotation rate for onset of elastic instability in the presence of viscous heating effects is thus given by

$$\frac{\lambda(\hat{T}_w)\omega_c}{\sqrt{\alpha}} = \mathcal{D}_{c0} + \frac{1}{K^2}\left(\frac{\eta_0(\hat{T}_0)\, e^{-\vartheta_w}\delta R^2\omega_c^2}{\hat{k}\hat{T}_0}\right), \tag{5.2}$$

where $\mathcal{D}_{c0}$ specifies the critical conditions for onset of the elastic instability under isothermal conditions and K captures the sensitivity of the stability boundary to the effects of viscous dissipation. Values of $\mathcal{D}_{c0}$ and K for representative values of β can be determined from Table 1.

As we have noted above, experimental trajectories through the parameter space of Fig. 6 are straight lines passing through the origin with slope $\sqrt{\alpha}\Theta$. For a given cone angle, there is thus a critical value of the thermoelastic parameter Θ_{max} beyond which the flow is completely stabilized. Assuming that the relationship above remains valid for moderate $\widetilde{Na} \geq 1$, this maximum value of Θ can be obtained from a tangency condition to be $\sqrt{\alpha}\Theta_{max} = K/(2\sqrt{D_{c0}})$. For the UCM model ($\beta = 1$) our computations give $K = 1.234$ and hence we find $\sqrt{\alpha}\Theta_{max} \approx 0.29$.

It should be noted that the value of Θ_{max} obtained here is related to that defined in [1] (which we denote $\Theta_{max}^{[RM]}$ for clarity) by $\Theta_{max}^{[RM]} = \Theta_{max}\sqrt{2/(1 + \theta_w/\delta)}$. The differences arise because of the radial averaging involved in $\widetilde{Na}$ and because the dimensionless thermal sensitivity (δ) of the Nahme model used in the present analysis is constant for all $\hat{T}_w$, whereas for the Arrhenius model used in [1] the thermal sensitivity is a weak function of the absolute temperature.

In Fig. 7 we show the expected variation in the stability boundary computed for conditions corresponding to the elastic fluid SM2 considered by Rothstein and McKinley [1]. For the conditions given we obtain $\mathcal{D}_{c0} = 5.48$ and $\sqrt{\alpha}\Theta_{max} = 0.279$. The shape of the resulting stability boundary is in good qualitative agreement with the experimental observations. A direct quantitative comparison with data is

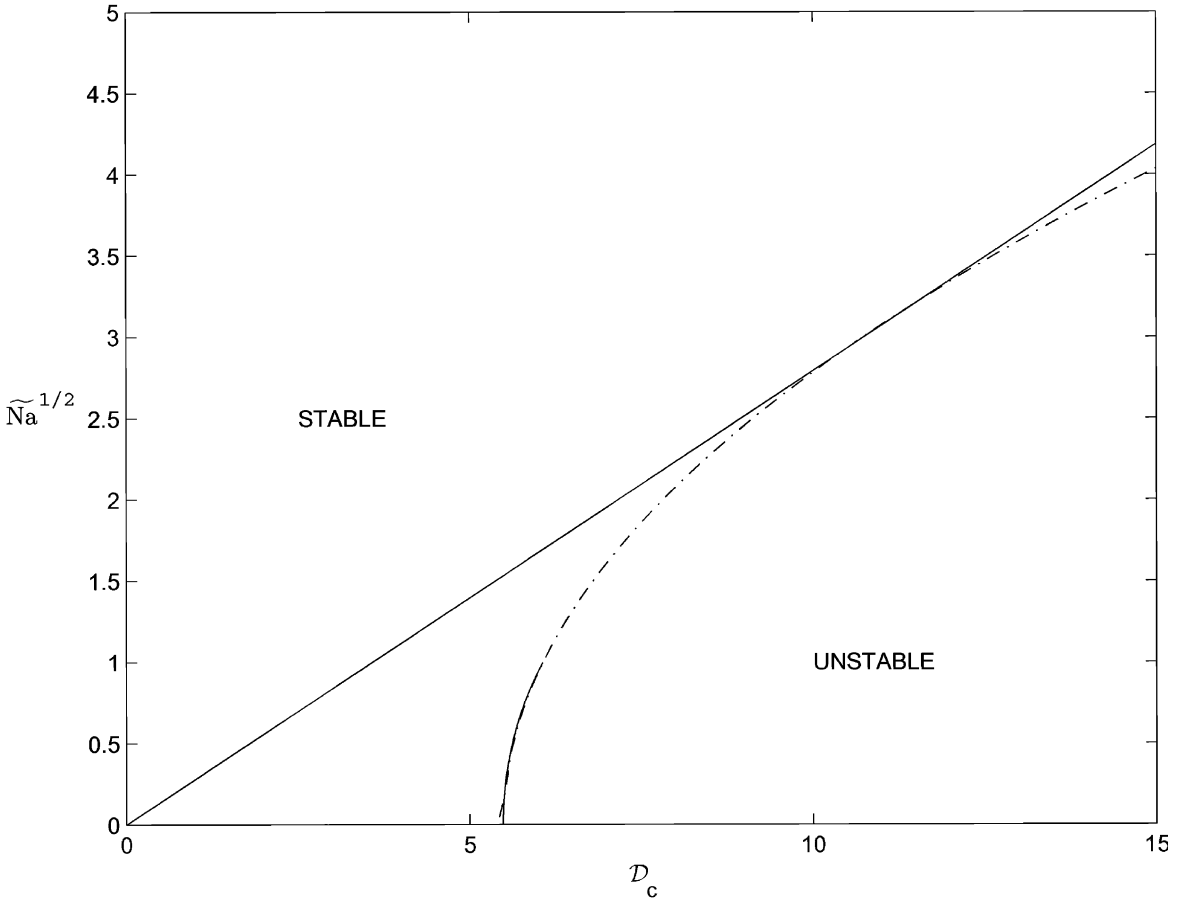

Fig. 7. Plot of $\mathcal{D}_c$ vs. $\widetilde{Na}^{1/2}$ extrapolated to moderate values of $\widetilde{Na}$, for $\mathcal{P} = 0$, $\beta = 0.26$, $\delta = 68$, and $\alpha = 0.035$. Here $\Theta_{max} = 1.49$.

not possible due to the importance of the discrete spectrum of relaxation times and the shear-thinning in the first normal stress coefficient documented in the experimental test fluid. Shear thinning serves to increase the critical Deborah number (or $\mathcal{D}_{c0}$) and would shift the computed stability boundary in Fig. 7 to the right. This leads to a significant difference (typically a factor of 5 or more) between the value of the critical Deborah number obtained experimentally and theoretically, even under isothermal conditions (see Fig. 7 of Rothstein and McKinley [1]). For a cone angle of $\alpha = 0.035$ and $\beta = 0.26$ the isothermal short wavelength theory gives $De_{c0} = 5.48 \times \sqrt{0.035} = 1.03$. In contrast, linear regression of the experimental data using the form shown in the inset to Fig. 6 gives $De_{c0} \cong 4.84$. If we assume that the parameter K is relatively unaffected by shear thinning in the fluid elasticity then the value of the parameter $\Theta_{max}^{[RM]}$ may be estimated from the present analysis to be

$$\Theta_{max}^{[RM]} \approx 0.279\sqrt{\frac{2}{1.057\alpha}}\left(\frac{De_{c0}^{theory}}{De_{c0}^{expt}}\right)^{1/2} \simeq 0.94.$$

This compares very favorably with the experimentally reported value of 0.92 computed by Rothstein and McKinley for the measured critical conditions and the appropriate (shear rate dependent) relaxation time $\lambda(\dot{\gamma}_{\text{crit}})$.

To summarize, we have considered the effects of viscous heating on the linear stability of axisymmetric disturbances in torsional flow of an Oldroyd-B fluid. The thermal sensitivity of the fluid is characterized by a dimensionless parameter δ (see Eq. (2.5)) which is typically large for polymeric fluids. The relevant dimensionless parameters governing the relative roles of viscoelasticity and viscous heating are the Deborah number and Nahme number, respectively. The asymptotic analysis in this paper is valid for the limits $Re \ll Na \ll 1$, $\alpha \ll 1$; and we neglect terms of order α^2; Na^2; $\alpha\, Na$; Na/δ, δ^{-1}. Exploratory calculations for moderate Peclet numbers (corresponding to $\mathcal{P} = Pe/De < 100$) did not reveal the presence of additional new disturbance modes and the numerical results in this paper have been presented for $\mathcal{P} = 0$ which closely approximates the experiments in [1]. In contrast to experiments and computations in the viscoelastic Taylor–Couette flow, the present computations show that viscous heating monotonically stabilizes the torsional base flow to both small and long wavelength disturbances. The magnitude of this stabilization increases the critical Deborah number approximately linearly with Na and is in good qualitative agreement with experimental observations [1]. Taking the ratio of these controlling parameters leads to a new thermoelastic parameter $\Theta = \sqrt{Na}/De$. This parameter is independent of the imposed kinematics and governs how significantly the results deviate from existing isothermal stability analyses of viscoelastic torsional flows (corresponding to $\Theta = 0$). The parameter Θ can be controlled by varying the fluid material properties or by varying the temperature imposed at the boundaries. This ability to systematically eliminate flow-induced elastic instabilities through control of additional thermophysical variables such as the imposed wall temperature may ultimately be of use in controlling the stability of polymer processing operations.

Acknowledgements

D.O. Olagunju was supported in part by NSF Grant # DMS 9704622. G.H. McKinley acknowledges support from the Schlumberger Foundation.

Appendix A

The coefficients appearing in Eqs. (4.2)–(4.4) are defined below, respectively, for the wave number $k = \mathrm{O}(1)$, and $k = \mathrm{O}(\alpha^{-1})$. For the sake of brevity terms of order $\mathrm{O}(\alpha)$, $\mathrm{O}(\delta^{-1})$ and $\mathrm{O}(\mu)$ have been omitted. Note that Ω is related to the growth rate σ by $\Omega = \sigma De$.

A.1. Moderate wave number

For the wave number $k = \mathrm{O}(1)$, the coefficients are

$$A_4 = (\beta\Omega - \Omega - 1) + \frac{1}{2}\widetilde{Na}\frac{[(\beta-1)(\Omega^2+2\Omega)-1](\psi^2-\psi)}{(\Omega+1)}, \tag{A.1}$$

$$A_3 = -\frac{1}{3}\beta\, De^2\, \widetilde{Na}\frac{(\Omega+3)\psi(\psi-1)(2\psi-1)}{(\Omega+1)^2} + \widetilde{Na}\frac{[(\beta-1)(\Omega^2+2\Omega)-1](2\psi-1)}{(\Omega+1)}, \tag{A.2}$$

$$A_2 = -2\beta\, De^2\, \frac{3(1+\mathrm{i}k) - 2\Omega^2 + \Omega(-3+\mathrm{i}k)}{(\Omega+1)^2} + \frac{1}{3}\beta\, De^2\, \widetilde{Na}\frac{(1+\mathrm{i}k)(\Omega+3)}{(\Omega+1)^2}$$

$$+ \beta De^2 \widetilde{Na}\frac{[\Omega^2 + 4\Omega(1+\mathrm{i}k) - 3(3+\mathrm{i}k)]\psi(\psi-1)}{(\Omega+1)^3} + \widetilde{Na}\frac{(\beta-1)(\Omega^2+2\Omega)-1}{(\Omega+1)}, \tag{A.3}$$

$$A_1 = \beta\, De^2\, \widetilde{Na}\frac{[(\Omega^2+4\Omega)(3+\mathrm{i}k) - 3(1+\mathrm{i}k)](2\psi-1)}{(\Omega+1)^3}, \tag{A.4}$$

$$A_0 = 0. \tag{A.5}$$

The remaining coefficients are

$$B_2 = 2\beta\, De^2 \frac{(\Omega+2)}{(\Omega+1)} + \frac{1}{6}\beta\, De^2\, \widetilde{Na}\frac{(12\psi^2 - 12\psi - \Omega^2 - 3\Omega - 2)}{(\Omega+1)^2}, \tag{A.6}$$

$$B_1 = 2\beta\, De^2\, \widetilde{Na}\frac{(2\psi-1)}{(\Omega+1)^2}, \tag{A.7}$$

$$B_0 = 0, \tag{A.8}$$

$$C_1 = -2\beta\, De^2 \frac{(\Omega+2)}{(\Omega+1)} + \frac{1}{3}\beta\, De^2\, \widetilde{Na}\frac{[(3\psi^2 - 3\psi + 1)(\Omega^2+3\Omega)+2]}{(\Omega+1)^2}, \tag{A.9}$$

and

$$C_0 = \beta\, De^2\, \widetilde{Na}\frac{\Omega(\Omega+3)(2\psi-1)}{(\Omega+1)^2}. \tag{A.10}$$

The coefficients in Eq. (4.3) are

$$D_2 = (\beta\Omega - \Omega - 1) + \frac{1}{2}\widetilde{Na}\frac{[(\beta-1)(\Omega^2+2\Omega)-1]\psi(\psi-1)}{(\Omega+1)}, \tag{A.11}$$

$$D_1 = \frac{1}{2}\widetilde{Na}\frac{[(\beta-1)(\Omega^2+2\Omega)-1](2\psi-1)}{(\Omega+1)}, \tag{A.12}$$

$$D_0 = 0, \tag{A.13}$$

$$E_3 = \frac{1}{6}\beta\, \widetilde{Na}\frac{\psi(\psi-1)(2\psi-1)}{(\Omega+1)}, \tag{A.14}$$

$$E_2 = \beta\frac{(\mathrm{i}k - 1 - 2\Omega)}{(\Omega+1)} - \frac{1}{12}\beta\widetilde{Na}\frac{(\mathrm{i}k - 5 - 2\Omega)}{(\Omega+1)} - \frac{1}{2}\beta\widetilde{Na}\frac{[3 - \mathrm{i}k + \Omega(1+\mathrm{i}k)](\psi^2-\psi)}{(\Omega+1)^2}, \tag{A.15}$$

$$E_1 = -\frac{1}{2}\beta\widetilde{Na}\frac{(\Omega(3+\mathrm{i}k) - 5 - 3\mathrm{i}k)(2\psi-1)}{(\Omega+1)^2}, \tag{A.16}$$

$$E_0 = 0, \tag{A.17}$$

$$F_1 = -(1 + \Omega - \beta\Omega) - \frac{1}{12}\widetilde{Na}\frac{[\Omega^2(1-\beta) + \Omega(2 - \beta + 6\beta\psi^2 - 6\beta\psi) + 1]}{(\Omega+1)}, \tag{A.18}$$

and

$$F_0 = -\frac{1}{2}\beta\widetilde{Na}\frac{\Omega(2\psi-1)}{(\Omega+1)}. \tag{A.19}$$

Lastly, the coefficients of Eq. (4.4) are

$$H_2 = -1, \tag{A.20}$$

$$H_0 = -\widetilde{Na}\frac{(\beta\Omega-\Omega-1)}{\Omega+1} + P\Omega, \tag{A.21}$$

$$G_1 = \beta\widetilde{Na}\frac{[3+3\mathrm{i}k+\Omega(-3+\mathrm{i}k)-2\Omega^2]}{(\Omega+1)^2} + P\widetilde{Na}(\psi-\psi^2), \tag{A.22}$$

$$G_0 = \tfrac{1}{2}P\widetilde{Na}(3+\mathrm{i}k)(2\psi-1), \tag{A.23}$$

and

$$K_1 = \widetilde{Na}\frac{(\beta\Omega-2\Omega-2)}{\Omega+1}. \tag{A.24}$$

A.2. Short wavelength limit

Here we have defined $k = \kappa/\alpha$, and $De = \mathcal{D}\sqrt{\alpha}$. The coefficients of Eq. (4.2) are

$$A_4 = \frac{\beta\Omega-\Omega-1}{\Omega+1} + \frac{1}{2}\widetilde{Na}\frac{[(\beta-1)(\Omega^2+2\Omega)-1]\psi(\psi-1)}{(\Omega+1)^2}, \tag{A.25}$$

$$A_3 = \widetilde{Na}(1-2\psi) + \beta\widetilde{Na}\frac{\Omega(\Omega+2)(2\psi-1)}{(\Omega+1)^2}, \tag{A.26}$$

$$\begin{aligned} A_2 = {} & -\kappa^2\left[2\frac{\beta\Omega-\Omega-1}{\Omega+1} + \widetilde{Na}\frac{[(\beta-1)(\Omega^2+2\Omega)-1](\psi^2-\psi)}{(\Omega+1)^2}\right] \\ & + \mathrm{i}\kappa\beta\mathcal{D}^2\left[-2\frac{(\Omega+3)}{(\Omega+1)^3} + \frac{1}{3}\widetilde{Na}\frac{[(1+3\psi^2-3\psi)(\Omega^2+4\Omega-3)+6]}{(\Omega+1)^4}\right] \\ & + \widetilde{Na}\frac{(\beta-1)(\Omega^2+2\Omega)-1}{(\Omega+1)^2}, \end{aligned} \tag{A.27}$$

$$A_1 = \beta\,\widetilde{Na}\,\mathcal{D}^2\mathrm{i}\kappa\frac{(\Omega^2+4\Omega-3)(2\psi-1)}{(\Omega+1)^4} - \kappa^2\,\widetilde{Na}\frac{((\beta-1)(\Omega^2+2\Omega)-1)(2\psi-1)}{(\Omega+1)^2}, \tag{A.28}$$

$$\begin{aligned} A_0 = {} & \widetilde{Na}\,\kappa^2\frac{((\beta-1)(\Omega^2+2\Omega)-1)(\psi^2-\psi)}{(\Omega+1)^2} \\ & - \kappa^4\left[\frac{\beta\Omega-\Omega-1}{\Omega+1} + \frac{1}{2}\widetilde{Na}\frac{((\beta-1)(\Omega^2+2\Omega-1))(\psi^2-\psi)}{(\Omega+1)^2}\right]. \end{aligned} \tag{A.29}$$

The others are

$$B_2 = 2\mathrm{i}\kappa\beta\mathcal{D}^2\frac{\Omega+2}{(\Omega+1)^2} + \frac{1}{6}\mathrm{i}\kappa\beta D^2\widetilde{Na}\frac{(12\psi^2-12\psi-\Omega^2-3\Omega-2)}{(\Omega+1)^3}, \tag{A.30}$$

$$B_1 = 2\mathrm{i}\kappa\beta\mathcal{D}^2\widetilde{Na}\frac{2\psi-1}{(\Omega+1)^3}, \tag{A.31}$$

$$B_0 = 0, \tag{A.32}$$

$$C_1 = -2\mathrm{i}\kappa\beta\mathcal{D}^2\frac{\Omega+2}{(\Omega+1)^2} + \mathrm{i}\kappa\beta\mathcal{D}^2\frac{1}{3}\widetilde{Na}\frac{[(3\psi^2-3\psi+1)(\Omega^2+3\Omega)+2]}{(\Omega+1)^3}, \tag{A.33}$$

and

$$C_0 = \mathrm{i}\kappa\beta\mathcal{D}^2\widetilde{Na}\frac{\Omega(\Omega+3)(2\psi-1)}{(\Omega+1)^3}. \tag{A.34}$$

The coefficients of Eq. (4.3) are

$$D_2 = \frac{\beta\Omega-\Omega-1}{\Omega+1} + \frac{1}{2}\widetilde{Na}\frac{((\beta-1)(\Omega^2+2\Omega)-1)(\psi^2-\psi)}{(\Omega+1)^2}, \tag{A.35}$$

$$D_1 = \frac{1}{2}\widetilde{Na}\frac{((\beta-1)(\Omega^2+2\Omega-1)(2\psi-1)}{(\Omega+1)^2}, \tag{A.36}$$

$$D_0 = -\kappa^2\left[\frac{\beta\Omega+\Omega-1)}{(\Omega+1)} + \frac{1}{2}\widetilde{Na}\frac{[(\beta-1)(\Omega^2+2\Omega)-1]}{(\Omega+1)^2}\right], \tag{A.37}$$

$$E_3 = 0, \tag{A.38}$$

$$E_2 = \frac{\beta}{(\Omega+1)^2} - \beta\frac{1}{12}\widetilde{Na}\frac{[(6\psi^2-6\psi)(\Omega-1)+\Omega+1]}{(\Omega+1)^3}, \tag{A.39}$$

$$E_1 = -\beta\frac{1}{2}\widetilde{Na}\frac{(\Omega-3)(2\psi-1)}{(\Omega+1)^3}, \tag{A.40}$$

$$E_0 = \beta\kappa^2\left[\frac{1}{12}\widetilde{Na}\frac{(6\psi^2-6\psi)(\Omega-1)+\Omega+1}{(\Omega+1)^3} - \frac{1}{(\Omega+1)^2}\right], \tag{A.41}$$

$$F_1 = -\frac{\beta\Omega-\Omega-1}{\Omega+1} - \frac{1}{12}\widetilde{Na}\frac{(1+\Omega)^2-\beta(\Omega^2+\Omega)+6\beta\Omega(\psi^2-\psi)}{(\Omega+1)^2}, \tag{A.42}$$

and

$$F_0 = -\frac{1}{2}\beta\widetilde{Na}\frac{\Omega(2\psi-1)}{(\Omega+1)^2}. \tag{A.43}$$

Finally, the coefficients of Eq. (4.4) are given by

$$H_2 = -1, \tag{A.44}$$

$$H_0 = \kappa^2 - \widetilde{Na}\frac{\beta\Omega-\Omega-1}{\Omega+1} + \mathcal{P}\Omega, \tag{A.45}$$

$$G_1 = \beta \widetilde{Na} \frac{\Omega + 3}{(\Omega + 1)^2}, \tag{A.46}$$

$$G_0 = \tfrac{1}{2} \mathcal{P} \widetilde{Na} (2\psi - 1), \tag{A.47}$$

and

$$K_1 = \widetilde{Na} \frac{\beta\Omega - 2\Omega - 2}{\Omega + 1}. \tag{A.48}$$

References

[1] J.P. Rothstein, G.H. McKinley, Non-isothermal modification of purely elastic flow instabilities in torsional flow of polymeric fluids, Phys. Fluids 13 (2) (2001) 382–396.
[2] R.M. Turian, R.B. Bird, Viscous heating in the cone-and-plate viscometer-II, Chem. Eng. Sci. 18 (1963) 689–696.
[3] L.E. Becker, G.H. McKinley, The stability of viscoelastic creeping plane shear flows with viscous heating, J. Non-Newtonian Fluid Mech. 92 (2000) 109–133.
[4] U.A. Al-Mubaiyedh, R. Sureshkumar, B.B. Khomami, Influence of energetics on the stability of viscoelastic Taylor–Couette flow, Phys. Fluids 11 (11) (1999) 3217–3226.
[5] J.M. White, S.J. Muller, Viscous heating and the stability of Newtonian and viscoelastic Taylor–Couette flows, Phys. Rev. Lett. 84 (22) (2000) 5130–5133.
[6] U.A. Al-Mubaiyedh, R. Sureshkumar, B. Khomami, Effect of viscous heating on the stability of Taylor–Couette flow, J. Fluid Mech., 2001, submitted.
[7] U.A. Al-Mubaiyedh, R. Sureshkumar, B. Khomami, Linear stability of viscoelastic Taylor–Couette flow: influence of fluid rheology and energetics, J. Rheol. 44 (5) (2000) 1121–1138.
[8] U.A. Al-Mubaiyedh, R. Sureshkumar, B. Khomami, Energetic effects on the stability of viscoelastic Dean flow, J. Non-Newtonian Fluid Mech. 95 (2/3) (2000) 277–293.
[9] R.M. Turian, Viscous heating in the cone-and-plate viscometer-III, Chem. Eng. Sci. 20 (1965) 771–781.
[10] F. Ding, A.J. Giacomin, R.B. Bird, C. Kweon, Viscous dissipation with fluid inertia in oscillatory shear flow, J. Non-Newtonian Fluid Mech. 86 (3) (1999) 359–374.
[11] R. Tanner, Engineering Rheology, 2nd Edition, Oxford University Press, Oxford, 2000.
[12] A. Avagliano, N. Phan-Thien, Torsional flow: elastic instability in a finite domain, J. Fluid Mech. 312 (1996) 279–298.
[13] D.O. Olagunju, Asymptotic analysis of the finite cone-and-plate flow of a non-Newtonian fluid, J. Non-Newtonian Fluid Mech. 50 (1993) 289–303.
[14] D.O. Olagunju, Effect of free surface and inertia on viscoelastic parallel plate flow, J. Rheol. 38 (1) (1994) 151–168.
[15] Y. Renardy, M. Renardy, A model equation for axisymmetric instability of small-gap parallel plate flow, J. Non-Newtonian Fluid Mech. 77 (1998) 103–114.
[16] L.M. Quinzani, R.A. Brown, G.H. McKinley, R.C. Armstrong, Modelling the rheology of polyisobutylene solutions, J. Rheol. 34 (1991) 705–748.
[17] D.O. Olagunju, L.P. Cook, Linear stability analysis of cone-and-plate flow of an Oldroyd-B fluid, J. Non-Newtonian Fluid Mech. 47 (1993) 93–105.
[18] N. Phan-Thien, Cone-and-plate flow of the Oldroyd-B fluid is unstable, J. Non-Newtonian Fluid Mech. 17 (1985) 37–44.
[19] A. Zebib, A Chebyshev method for the solution of boundary value problems, J. Comp. Phys. 53 (1984) 443–455.
[20] A. Zebib, Removal of spurious modes encountered in solving stability problems by spectral methods, J. Comp. Phys. 70 (1987) 521–525.
[21] D.O. Olagunju, Elastic instabilities in cone-and-plate flow: small gap theory, ZAMP 46 (1995) 946–959.
[22] G.H. McKinley, J.A. Byars, R.A. Brown, R.C. Armstrong, Observations of elastic instability in cone-and-plate and parallel-plate flows of polyisobutylene Boger fluid, J. Non-Newtonian Fluid Mech. 40 (1991) 201–229.
[23] G.H. McKinley, A. Oztekin, J.A. Byars, R.A. Brown, Self-similar spiral instabilities in elastic flows between a cone and a plate, J. Fluid Mech. 285 (1995) 123–164.